

# **Modeling a Three-dimensional River Plume over Continental Shelf Using a 3D Unstructured Grid Model**

**Ralph T. Cheng**  
**U. S. Geological Survey**  
**Menlo Park, California**

**Vincenzo Casulli**  
**Department of Civil and Environmental Engineering**  
**University of Trento**  
**Trento, Italy**

## **Abstract**

River derived fresh water discharging into an adjacent continental shelf forms a trapped river plume that propagates in a narrow region along the coast. These river plumes are real and they have been observed in the field. Many previous investigations have reported some aspects of the river plume properties, which are sensitive to stratification, Coriolis acceleration, winds (upwelling or downwelling), coastal currents, and river discharge. Numerical modeling of the dynamics of river plumes is very challenging, because the complete problem involves a wide range of vertical and horizontal scales. Proper simulations of river plume dynamics cannot be achieved without a realistic representation of the flow and salinity structure near the river mouth that controls the initial formation and propagation of the plume in the coastal ocean. In this study, an unstructured grid model was used for simulations of river plume dynamics allowing fine grid resolution in the river and in regions near the coast with a coarse grid in the far field of the river plume in the coastal ocean. In the vertical, fine fixed levels were used near the free surface, and coarse vertical levels were used over the continental shelf. The simulations have demonstrated the uniquely important role played by Coriolis acceleration. Without Coriolis acceleration, no trapped river plume can be formed no matter how favorable the ambient conditions might be. The simulation results show properties of the river plume and the characteristics of flow and salinity within the estuary; they are completely consistent with the physics of estuaries and coastal oceans.

## **I. Introduction**

River derived fresh water discharging into an adjacent continental shelf forms a trapped river plume that propagates in a narrow region along the coast. These river plumes are real and they have been observed in the field (Hicky et al., 1998; Berdeal et al, 2002; Fong and Geyer, 2002). The trapped river plumes transport fresh water, nutrients, and pollutants over a large coastal region that could affect the regional ecosystem. A trapped river plume can propagate for hundreds of kilometers. The importance of the river plume dynamics prompted numerous past and present investigations. Because the region of interest is very large, direct measurements of water properties over such a large domain of interest are quite difficult. Although satellite images can provide evidence of the presence of river plumes, their properties are somewhat qualitative. Therefore numerical modeling has become a powerful tool in the investigations of trapped river plume dynamics.

Using a relatively coarse grid, Chao and Boicourt (1986) modeled the coastal ocean assuming a constant depth basin of limited extent. Neither tidal motions nor ambient currents were used. At the

river mouth, estuarine circulation was artificially imposed in the form of a boundary condition. Although the numerical model was crude by today's standard, their model reproduced essential features of a trapped river plume. In a follow up paper, Chao (1988) added the effects of a sloping bottom in the ocean. Hyatt and Signell (2000) used a Princeton Ocean Model (POM) (Blumberg and Mellor, 1987) over a variable grid mesh to represent the coastal ocean with a sloping bottom. The river was modeled as a simple fresh water source discharging into the coastal ocean. Neither tides nor wind forcing was used. In order to reproduce the essential features of the river plume, an ambient current of 5 cm/sec was imposed in the direction of Kelvin wave propagation; i.e. anticyclonically in the northern hemisphere. The convective transport of fresh water would mimic that of a trapped river plume. It is not clear whether a trapped river plume would be formed if an ambient current were not introduced. However, Hyatt and Signell (2000) emphasized that the objective of their study was on the investigation of a few numerical convective schemes used in the numerical model.

Garvine (1999, 2001) has studied trapped river plumes since the mid-1980; main results of Garvine's findings are summarized in these two papers. Through dimensional analysis, Garvine (1999) pointed out that the properties of a trapped river plume are functions of river width, depth, discharge, exiting velocity, degree of stratification (mixing in the vertical water column), intensity of Coriolis acceleration (latitude of the river), bottom slope of the coastal ocean, winds, and upwelling and downwelling of coastal currents. Although Garvine's studies were comprehensive and extensive, there are some weaknesses in the numerical model that produced these conclusions. In Garvine's model (1999), the river was represented as a fresh water source without tidal motion. The flow and salinity structures near the river mouth play a very important role in the eventual formation and propagation of the fresh water plume along the coast. Proper simulations of river plume dynamics cannot be achieved without a realistic representation of the flow and salinity structure near the river mouth. When the tides are neglected, the simulations are equivalent to reproducing residual flow and salinity transported by residual currents. While this approach might be justifiable, a proper turbulence closure should be used to represent the vertical mixing in a residual time scale. Therefore, if the dynamics in tidal time-scale is not considered, the adaptation of Mellor-Yamada closure in residual calculations is questionable.

Garvine (1999, 2000) also used POM (Blumberg and Mellor, 1987) in his investigations. The turbulence closure scheme was based on the Mellor-Yamada 2.5 level model (1982). In most of the simulations, tidal motions were neglected, and yet the kinetic energy based Mellor-Yamada 2.5 turbulence closure was used. Therefore the turbulent mixing in the vertical was not properly represented in these simulations. Since there was no direct measurement of river plume properties that can be used for comparison with model simulations, it is hard to judge the correctness of the model results. In real world situations, tidal motions are always present and important. It is important to note that the Mellor-Yamada turbulence closure is derived from the balance of turbulent kinetic energy (TKE), production and dissipation of TKE, and the transport of a local mixing length. When the tides are neglected, the simulations represent temporal variations of residual currents not the kinetic energy associated with tidal currents; thus the use of the Mellor-Yamada closure in the 'residual' model might be, at least, questionable. In the end, the results reported by Garvine (1999, 2001) are likely to be qualitatively correct; a quantitative capturing of the plume properties is not yet available.

Other investigations also used numerical models to examine the driving mechanisms and the balance of momentum of a river plume (Zhang et al, 1987; Garvine, 1987; Chao, 1988; O'Connor, 1990; Oey and Mellor, 1993; Kourafalou et al, 1996; Yankovsky and Chapman, 1997; Berdeal et al, 2002, and Fong and Geyer, 2002). Nearly all the models assumed the river inflow as a freshwater source and neglected the astronomical tides. Most models also assumed a constant depth ocean. They investigated the resulting transport of a low salinity plume driven by upwelling or downwelling due to the superimposing wind forcing. Quite often an ambient coastal current had to be imposed in order to reproduce the transport of freshwater in a river-derived plume. Numerical modeling of the dynamics of river plumes is very challenging because the complete problem involves a wide range of vertical and horizontal scales. A typical river is about 10 - 20 m deep, a few kilometers wide, and up to a hundred of kilometers long, while over the continental shelf, the water is a few hundred meters deep and the region of interest is a few hundred kilometers in length. Many authors represent the plume problem by a simple source function and justify such a representation by stating that "The establishment of a realistic estuarine flow which requires a much larger channel is beyond the scope of the present study." for example, Kourafalou et al (1996).

In this study, an advanced 3D numerical model known as UnTRIM (Casulli and Walters, 2000; Casulli and Zanolli, 2002; Cheng and Casulli, 2002) is used in simulations of a river plume. The numerical model uses an unstructured grid in the computations that allow the use of a very high-resolution model grid to study the mechanisms that are responsible for the formation of a river plume over the continental shelf, and the use of coarse grids for far field to allow extensive coverage of coastal-ocean. In the vertical, fine fixed levels are used in surface layers in the top 20 m, and coarse vertical levels are for the remaining domain covering the continental shelf. The main objective of this study is to show the correct physics with which the formation and propagation of a trapped freshwater plume in the coastal ocean. In addition, the properties of the river plume are related to the circulation structure in the river-estuary-ocean system, and the circulation near the mouth of estuary (river).

## **II. The UnTRIM Numerical Model**

One of the common characteristics of the TRIM family of models is that the numerical solutions are computed in physical space without any coordinate transformation in the x-, y-, or z-directions. Semi-implicit finite-difference schemes are used to control the propagation of surface gravity waves that could cause numerical instability (Casulli, 1990; Casulli and Cheng, 1992; Casulli and Cattani, 1994). The latest addition to the TRIM family of models uses an orthogonal unstructured grid while a semi-implicit finite-difference method is still used for solving the 3D shallow water equations (Casulli and Walters, 2000; Casulli and Zanolli, 1998, 2002). The combined use of a semi-implicit algorithm for stability and an unstructured grid for flexibility in solving the shallow water equations constitutes the essence of the UnTRIM model. The governing equations include the 3D conservation equations of mass, momentum, a transport equation for each scalar variable, an equation of state, and a kinematic free-surface equation. The estuarine and coastal system is assumed to be sufficiently large so that a constant Coriolis acceleration term is included in the momentum equations. Furthermore, the water is assumed to be incompressible; the pressure is assumed to be hydrostatic; and the Boussinesq approximation applies. Cheng and Casulli (2002) has reported an evaluation of the UnTRIM model for applications to estuarine and coastal circulation; the details of the governing equations and solution algorithm are referred to Casulli and Walters( 2000), Casulli and Zanolli, (2002) and Cheng and Casulli (2002).

### III. Turbulence closure

For three-dimensional barotropic flows (constant density), the solute transport equation is uncoupled from the momentum equations. For baroclinic flows, the transport equations are coupled with the momentum equations through the density gradient terms and the choice of a turbulence closure sub-model. All transport variables including salinity, temperature, and turbulence properties among others are solved lagged one time-step. Thus, the baroclinic forcing terms (density gradients) in the momentum equations are effectively solved explicitly, resulting in a numerical scheme that is subjected to a weak Courant-Friedrich-Lewy (CFL) stability condition based on the propagation of internal waves. Turbulence transport equations are solved in a similar manner; the resulting turbulence closure properties do not affect the numerical stability of the solution scheme as long as the effective vertical eddy viscosity remains non-negative. A non-negative bottom friction coefficient is typically specified by the Manning-Chezy formula, or by fitting to a bottom turbulent boundary layer.

Vertical mixing mechanism and the resulting stratification near the mouth of an estuary is an important aspect of the river plume dynamics; the correct choice of a turbulence closure sub-model is necessary in order to properly reproduce the freshwater stratification near the mouth of the estuary and the gravitational circulation within the estuary/river. A stratified ambient condition just out side of the river mouth creates a favorable condition for the formation of a freshwater river plume that is forced by Coriolis acceleration, resulting in trapping of a thin freshwater layer along the coast in the direction of Kelvin wave propagation. Because the horizontal length scale in the mixing process is several orders of magnitude larger than the length scale of vertical mixing, the horizontal eddy viscosity and diffusivity play a less important role. Several different approaches have been reported for treating vertical eddy viscosity,  $N_v$ , and vertical diffusivity,  $K_v$ , with varying degrees of success. The  $k$ - $\epsilon$  type of closure is commonly used in the European modeling community (Rodi, 1984; Uittenbogaard et al., 1992). Direct field verifications of the  $k$ - $\epsilon$  closure in estuaries are rare.

Two types of turbulence closure sub-models have been implemented for the present model application. For a type I closure model, the vertical eddy and diffusivity coefficients are written as neutral (unstratified) mixing coefficients modified by a damping function due to stratification. Thus,

$$N_v = N_o \psi_N(Ri) \quad \text{and} \quad K_v = K_o \psi_K(Ri) \quad (1)$$

where  $N_o$  and  $K_o$  are the neutral values of eddy viscosity and diffusivity coefficients;  $Ri$  is a local gradient Richardson number,

$$Ri = -\frac{g}{\rho} \frac{\frac{\partial \rho}{\partial z}}{\left[ \left( \frac{\partial u}{\partial z} \right)^2 + \left( \frac{\partial v}{\partial z} \right)^2 \right]} \quad (2)$$

and  $\psi_N(Ri)$  and  $\psi_K(Ri)$  are damping functions. In Eq.(2),  $\rho$  is density,  $g$  is gravitational acceleration,  $\frac{\partial \rho}{\partial z}$  is the vertical density gradient, and  $\left[ \left( \frac{\partial u}{\partial z} \right)^2 + \left( \frac{\partial v}{\partial z} \right)^2 \right]^{1/2}$  is the velocity gradient in

vertical direction. Based on theoretical arguments or empirical data, the damping functions are given in a variety of forms usually dependent on the local gradient Richardson number. Table I gives some commonly used type-I turbulence closure models including the constant value (CV) model, the classic Munk-Anderson (MA) formulation (1948) of the damping function, and the turbulence models proposed by Lehfeldt and Bloss (LB) (1988), and Pacanowski and Philander (PP) (1981). The turbulence models LB and PP have been used in a study of periodic stratifications in San Francisco Bay (Cheng and Casulli, 1996).

Table I. Some Turbulence Closure Models  
(  $N_v = N_o \psi_N$  and  $K_v = K_o \psi_K$  )

Mixing Model	$N_o$ (m <sup>2</sup> /sec)	$K_o$ (m <sup>2</sup> /sec)	$\psi_N$	$\psi_K$	Remarks
Constant (CV)	0.0001 ~0.001	0.0001 ~0.001	1.0	1.0	No Ri dependence
Munk & Anderson (MA)	$N_o$	$K_o$	$(1+10Ri)^{-1/2}$	$(1+3.33Ri)^{-3/2}$	
Lehfeldt & Bloss (LB)	$l^2 \left  \frac{\partial u}{\partial z} \right $	$l^2 \left  \frac{\partial u}{\partial z} \right $	$(1+3Ri)^{-1}$	$(1+3Ri)^{-3}$	$l = \kappa z(1-z/H)^{1/2}$
Pacanowski & Philander (PP)	0.01	$K_o$	$(1+3Ri)^{-2}$	$(1+3Ri)^{-1}$	

The neutral values of eddy viscosity and diffusivity are taken from a mixing length turbulence model from Rodi (1984),

$$N_o = K_o = (C'_\mu)^3 / C_d)^{1/2} l^2 |dU/dz| \quad \text{with} \quad l = \kappa z(1-z/H)^{1/2} \quad (3)$$

where  $C'_\mu = 0.58$ ,  $C_d = 0.1925$  and  $l$  is the mixing length,  $\kappa$  is von Karman constant,  $z$  and  $H$  are the distance from bed and the total water depth, respectively.

Type-II turbulence closure models consider the transport of mixing length, turbulent kinetic energy, and dissipation. The k- $\epsilon$  model and the model proposed by Mellor-Yamada (1982) fall in this category. When a higher level of physical processes is considered, the turbulent eddy viscosity and diffusivity must be solved along with the flow variables, thus incurring higher computational expense. As reported in the literature, all models have reproduced certain flow conditions with some degree of success. In this study, a Mellor-Yamada 2.5 level turbulence closure scheme has been implemented in the UnTRIM model. The turbulent kinetic energy ( $q^2/2$ ) and the quantity ( $q^2 l$ ) are solved from transport equations for  $q$  and  $l$ . The vertical eddy viscosity and diffusivity are then defined as functions of ( $ql$ ), and stability functions are derived by Mellor-Yamada (1982). Details of the Mellor-Yamada 2.5 level

turbulence closure sub-model and its stability functions are well documented, they are not repeated here.

#### IV. Model configuration of a river and coastal ocean system

Since the main objective of this study is to show the interactions of river/estuarine flows with the coastal ocean, both the coastal ocean and the connecting river/estuary must be well represented. An estuary (river) with a constant depth of 20 m, 80 km long and 4 km wide is assumed. The coastal ocean is 140 km x 440 km with the river located at 120 km north from the southern boundary of the ocean, Figure 1. The coastal ocean has a constant slope; the water depth varies from 20 m at shore to 200 m at the western boundary of the study region. An  $M_2$  tide of 1 m amplitude is specified at the western ocean open boundary where the salinity is 30 ppt. At the northern and southern open boundaries of the ocean, a zero normal gradient for all variables are assumed. At shorelines, the normal velocity is zero, and at the head of the river an open boundary is used, where a constant stage is assigned.

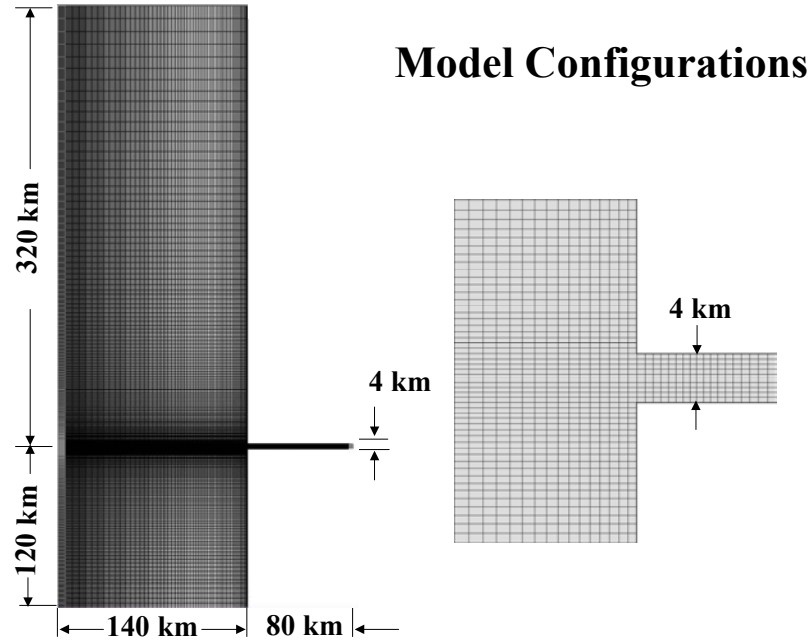


Figure 1. A river/estuary of 4 km wide, 80 km long and 20 m deep is connected to a coastal ocean of 140 km x 440 km. Depth in the ocean varies from 20 m at shore to 200 m at 140 km from shore.

Furthermore, at all open boundaries, a radiation boundary condition

$$\frac{\partial \eta}{\partial t} + \frac{\partial}{\partial x} \left[ \int_{-h}^{\eta} u dz \right] + \frac{\partial}{\partial y} \left[ \int_{-h}^{\eta} v dz \right] = (\eta^* - \eta) / \tau_{\text{rex}} \quad (4)$$

is applied, where  $\eta^*$  is the specified water level, and the actual water level  $\eta$  is determined by Eq.(4). In Eq.(4),  $(u,v)$  are velocity components in  $(x,y)$  directions;  $h$  is water depth, and  $\tau_{\text{rex}}$  is the specified relaxation time. At the head of the river, salinity is assumed to be 0 ppt. For a given water level at the

head of the river, the net river discharge is not known a priori. The tide propagating from the open ocean into the estuary is allowed to pass through the head of the river (radiation boundary condition); the entire river reach is influenced by tidal fluctuations. Due to tides, the volumetric flux of water in a river cross-section is a function of time. The net river discharge is the tidally averaged volumetric flux, which is determined during the simulation.

The UnTRIM model performs computations over an unstructured orthogonal grid-mesh. A combination of three-sided or four-sided polygons can be used. To assure orthogonality, a variable sized rectangular computational mesh shown in Figure 1 is used. The river-ocean interactions are expected to be most intense near the river mouth, therefore a very fine mesh is used in this region. A fine mesh is also used along the coast of the ocean. A coarse grid-mesh is used for regions away from the river mouth to optimize computing time because the river-ocean interactions are expected to decrease with distance from the river mouth. The computational grid has 125 node-points in the east-west direction and 200 points in the north-south direction. Excluding dry points, there is a total of 13,471 nodes on the horizontal plane. Fixed z-levels are used to represent the model domain in the vertical. In order to capture the thin fresh water lens, the vertical levels are defined in finer intervals near the free surface, and distributed more sparingly in deep water so that the z-levels are located at  $z = 0.5, 1.0, 2.0, 4.0, 6.0, 8.0, 10.0, 12.0, 14.0, 16.0, 18.0, 20.0, 23.0, 27.0$  m,...etc. A total of 30 layers is used to cover the ocean up to 200 m. Within the top 20 m, 12 layers are used to resolve the vertical structure of the dependent variables. The overall grid-mesh includes 262,846 3D computational cells.

The velocities are assumed to be zero initially, and the salinity varies from 30 ppt at the western boundary of the ocean to 0 ppt at the head of the river. Initially the salinity distribution in space is obtained by linear interpolation between these two extreme values. During simulations computed results of all dependent variables are saved at selected intervals (every 2 hours). Time-series of the dependent variables are saved at pre-selected stations. At each station, time-series of the 3D velocity and salinity structures, depth-averaged velocity (speed and direction), salinity, and the water level are recorded for further analysis.

## V. Results

### A. Choice of turbulence closure sub-model and net river discharge

The entire coastal ocean and estuary system is driven by the tides at ocean boundaries and by river outflow. Figure 2 shows a typical example of the time-series of depth-averaged salinity, sea-level, depth-averaged speed and direction at two stations 30 km (dotted line) and 50 km (solid line) from the head of the river. The tidal current speed varies from  $\sim 75$  cm/sec (flood) to  $\sim -100$  cm/s (ebb), and the tidal current direction is nearly bi-directional. The salinity fluctuates with the tide, with the mean salinity value decreasing as the station is located closer to the head of the river. Most previous numerical studies of trapped river plumes neglected the tides; the river discharge was represented by a freshwater source. The circulation in the modeled estuary was the residual current with which the salinity was transported. This formulation may give rise to a qualitatively correct description of the plume if a correct turbulence sub-model representing the mixing processes at the residual time scales was used. Clearly the kinetic energy distribution and its temporal variations, along with the spatial distribution of velocity shear, dissipation and production of turbulence in a residual time-scale would differ by an order of magnitude when examined in a tidal time-scale. As previously noted, the Mellor-Yamada 2.5 level turbulence closure is based on the transport of turbulent kinetic energy ( $q^2/2$ ) and a length scale quantity ( $q^2 l$ ), this sub-model should only be used

in simulations of tidal time-scale processes. When the Mellor-Yamada 2.5 level sub-model is used in simulations of residual processes, the correct physics are NOT represented in the computations, and the model results are suspect.

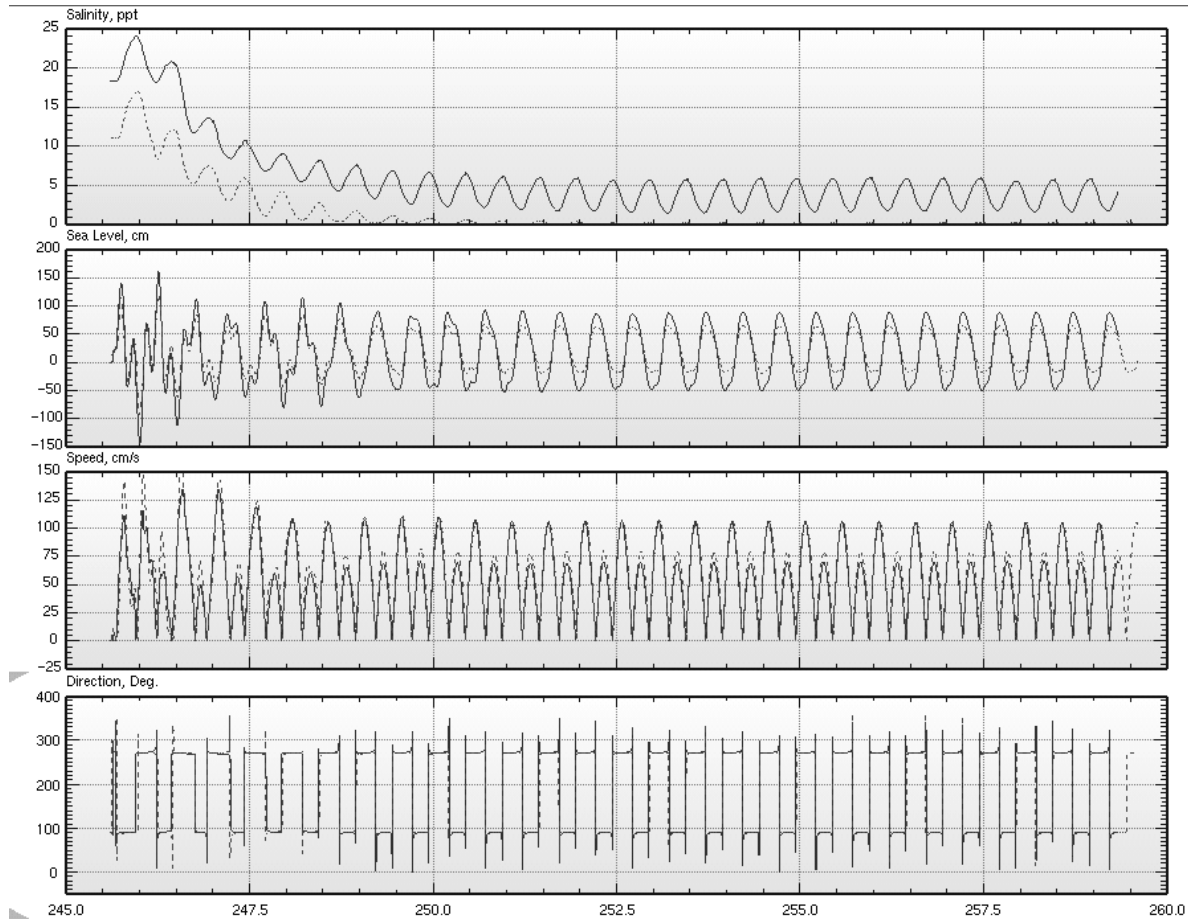


Figure 2. Time-series of depth averaged salinity, sea-level, speed and direction at two stations 30 km (dotted line) and 50 km (solid line) from the head of the river.

Figure 3 shows the instantaneous volumetric flux at a cross section 20 km from the head of the river. Positive values indicate upstream pointing flux. The tidal fluctuations give volumetric fluxes on the order of  $5.0 \times 10^4 \text{ m}^3/\text{s}$ , while the low pass-filtered net flux converges to  $7.2 \times 10^3 \text{ m}^3/\text{s}$ . It is reasonable to expect the tidal volumetric flux to be an order of magnitude larger than the net flux (residual). For each simulation, a stage level at the head of the river is specified; the net river discharge is determined in the course of simulation.

## B. Coriolis forcing

Coriolis acceleration is the main driving force responsible for the formation of trapped river plumes; all other factors such as tides, river discharge, and turbulence mixing acting together in the ocean-estuary system are responsible for creating a condition conducive to the formation of a trapped plume. However, without Coriolis forcing, the mechanism for the formation of river plume does not exist. To demonstrate this assertion, several simulations were carried out using a range of river



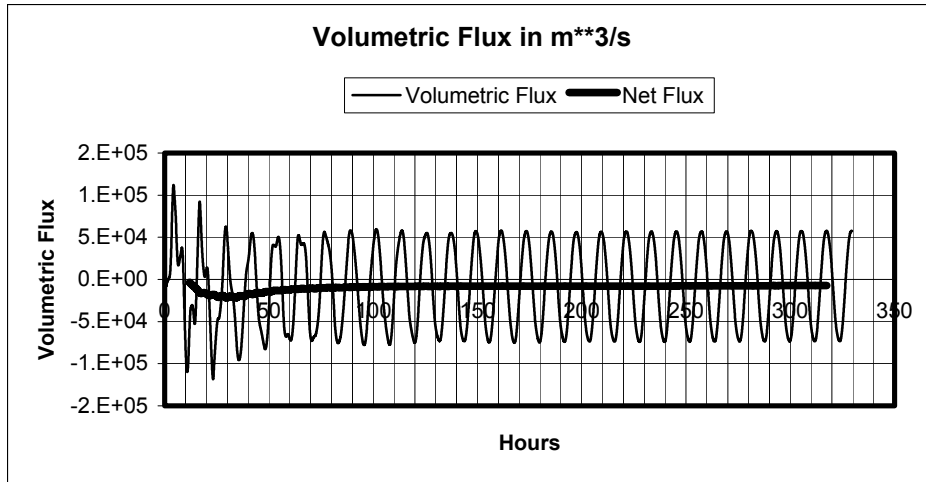


Figure 3 Instantaneous volumetric flux passing a cross-section of the river is on the order of  $5.0 \times 10^4 \text{ m}^3/\text{s}$ , while the low pass-filtered net flux converges to  $7.2 \times 10^3 \text{ m}^3/\text{s}$ , an order of magnitude smaller.

values and without Coriolis forcing. A symmetrical freshwater plume is seen in the region adjacent to the mouth of the river. In a few days, the mean-size of the plume appears to have reached a steady state although small fluctuations can be observed as the flooding and ebbing processes progress in time. The size of the freshwater zone is a function of river discharge, but under none of these scenarios was a trapped river plume along the coast found. Shown in Figure 4 is the symmetric freshwater zone along with the depiction of the velocity field for a medium river discharge value.

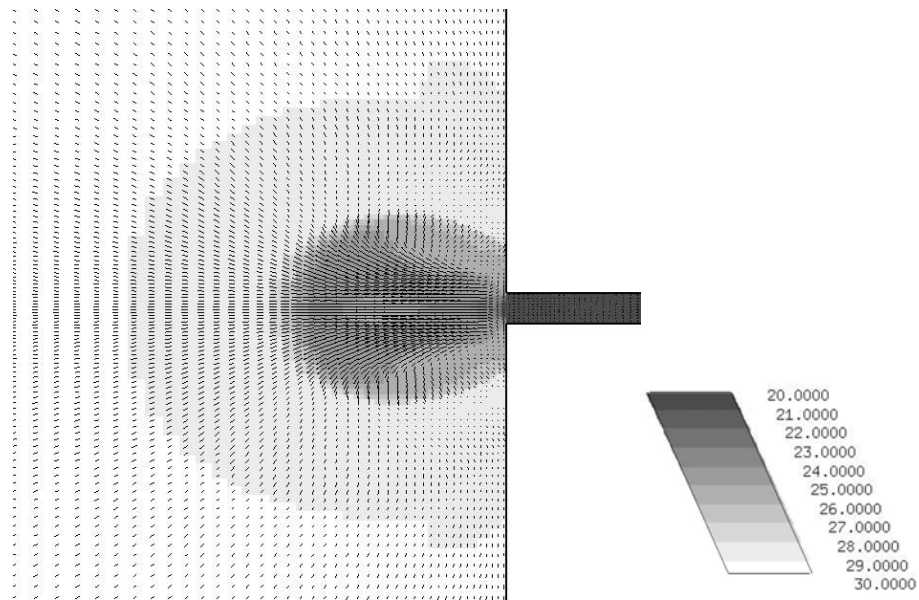


Figure 4. The symmetrical pattern of freshwater region is shown near the river mouth, where the black and white shade scheme displays only salinity between 20 and 30 ppt with lighter shade representing higher salinity. The velocity distribution is also symmetric with respect to the axis of the estuary.

It is instructive to examine the cycle of tidal circulation near the river mouth. The velocity field just outside of the river mouth assumes a “jet-like” flow distribution during an ebbing cycle, with high momentum flow exiting along the direction of the river axis resembling a jet flow. The intensity of momentum decreases away from the centerline of the main jet and away from the river mouth. During flood, the velocity field behaves as a “sink” flow; the momentum is roughly evenly distributed as flow entering into the estuary from all directions. Because of the net river discharge as well as vertical stratification, the exiting momentum in the surface layer (ebbing) is substantially higher than the momentum of the returning flow (flooding). Both the ebb dominance of flows and the distinctly different patterns of momentum distribution between flooding and ebbing cycles have direct bearings on the formation of trapped river plumes. In the northern hemisphere, Coriolis acceleration forces the flow to bend clockwise; the magnitude of the acceleration is proportional to the magnitude of the velocity itself ( $\vec{\Omega} \times \vec{V}$ ), Figure 5. During ebb, the high momentum “jet-like” flow is pushed clockwise with a maximum acceleration. During flood, the Coriolis acceleration acts more evenly because the momentum distribution is more even (sink flow). When the momentum is weak, the Coriolis acceleration still plays a role, however, the net effect of Coriolis acceleration is proportionally weak.

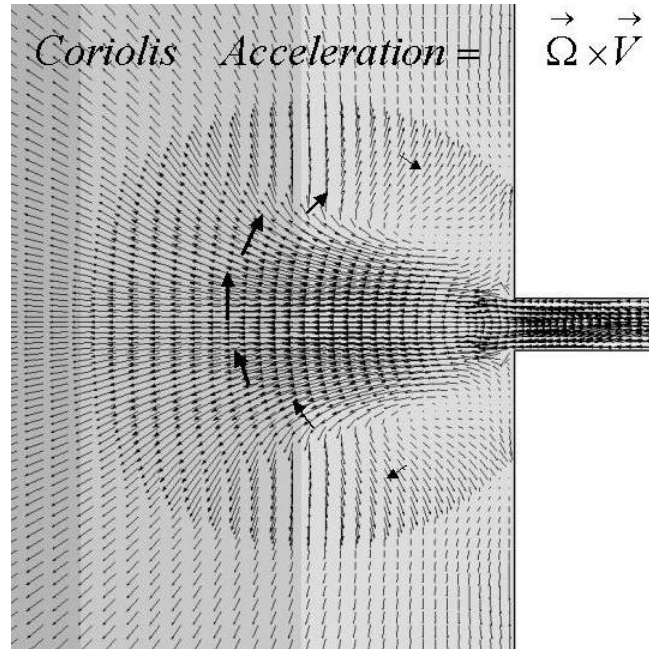


Figure 5. Schematic diagram illustrates the properties of Coriolis acceleration (arrows normal to velocities) in an ebbing cycle with flow exiting from the mouth of the estuary.

Figures 6a-6f show the surface velocity distribution at the mouth of the estuary for a tidal cycle (12 hours). Over a tidal cycle, the dominating exiting flow is pushed first to the north and then landward against the coast north of the river mouth, forming a trapped river plume. The residual circulation south of the river mouth spreads freshwater at a much slower rate, Figure 7. After 14 days into the simulation, the surface freshwater plume is shown propagating to the north trapped in a coastal zone by Coriolis acceleration. Some freshwater is transported south starting from a mixing zone near the south-side of the estuary. The southward transporting freshwater is NOT trapped to the coast by Coriolis acceleration, and is spreading over a broader region.

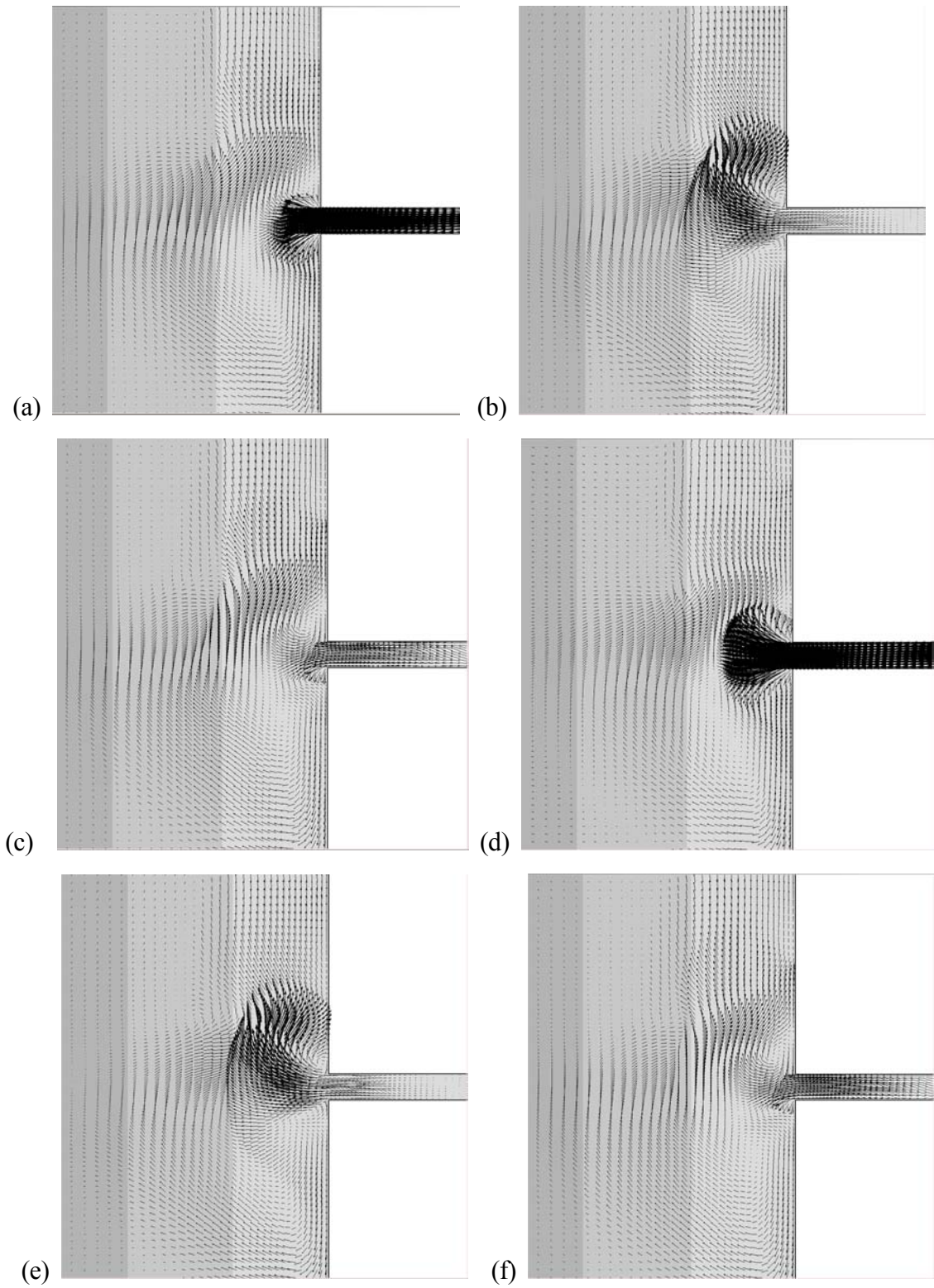


Figure 6. Surface velocity distribution near the mouth of an estuary over a 12-hour cycle. Each snapshot of the velocity distribution is taken at 2-hour interval.

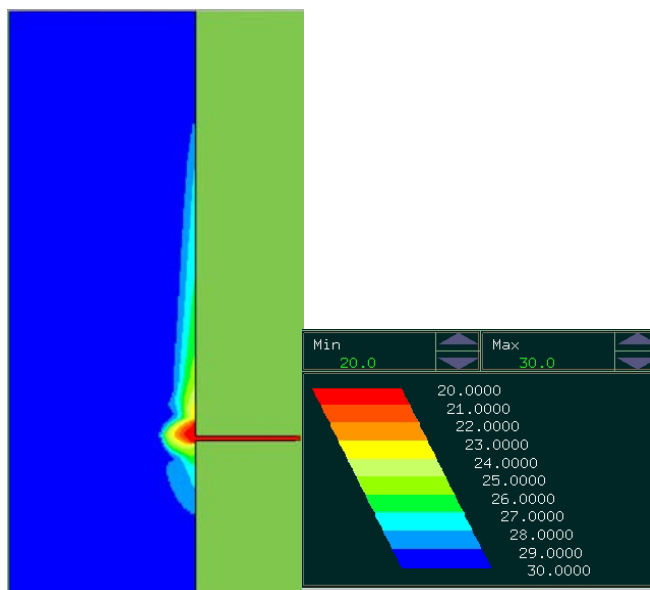


Figure 7. Trapped surface river plume at medium river discharge ( $7.2 \times 10^3 \text{ m}^3/\text{s}$ ) 14 days into the simulation. The color scheme for surface salinity ranges between 20 and 30 ppt with lighter shade representing higher salinity.

### C. River Discharge

Although the principal mechanism for the formation of a trapped river plume is Coriolis forcing, other parameters determine the gross properties of the trapped plume. Turbulence mixing controls the development of vertical stratification. Highly stratified flow near the river mouth concentrates higher momentum in the surface layer; such a condition is more conducive to the development of trapped river plumes. Of the few turbulence sub-models discussed in Section III, if type-I closure models were used, the estuary would tend to be well mixed. Of course, this situation could also be adjusted by changing the coefficients in the closure models. While there is no analytical solution for this problem to guide calibration of the model, the type-II Mellor-Yamada 2.5 level turbulence closure sub-model was used for all remaining simulations. This closure was used because the sub-model includes more complete consideration of the mixing mechanisms. Numerical simulations were conducted for three river discharges ranging from low ( $1.6 \times 10^3 \text{ m}^3/\text{s}$ ), medium ( $7.2 \times 10^3 \text{ m}^3/\text{s}$ ) to high ( $10.6 \times 10^3 \text{ m}^3/\text{s}$ ) flows. In all cases, the gross properties of the trapped river plume show the same pattern but differ quantitatively. The simulated properties of the river plumes after 14 days are summarized in Figures 8 and 9. The higher the river discharge, the further the trapped freshwater plume propagates northward. The “bulged head” of the river plume is also proportional to river discharge. The transport of fresh water to the south of the river mouth shows similar properties except the freshwater spreads over a broader region. This region grows with increasing river discharge. Within the estuary, the river discharge interacts with tides to determine the location of the salt-water front in the estuary. In a tidal cycle, the location of 2 ppt salinity moves toward the mouth during the ebbing cycle, and moves toward the head of the river during flood. The tidal cycle mean location of the salt-water front (represented by the location of 2 ppt) is determined to be a function of river discharge, Figure 9. The salinity distribution in the vertical cross-section of the estuary-coastal-ocean system is shown in Figure 9 in which the salinity values are depicted in black and white shades between 0.0 and 30 ppt. The locations of 2 ppt varies from 58.5km, 35 km, and 25

km for the respective low ( $1.6 \times 10^3 \text{ m}^3/\text{s}$ ), medium ( $7.2 \times 10^3 \text{ m}^3/\text{s}$ ), and high ( $10.6 \times 10^3 \text{ m}^3/\text{s}$ ) river discharges. Near the mouth of the estuary, an upwelling advection cell develops and intensifies with higher river discharge to counter-balance the exiting fresh water momentum flux from the river.

### Trapped River Plume after 14 days:

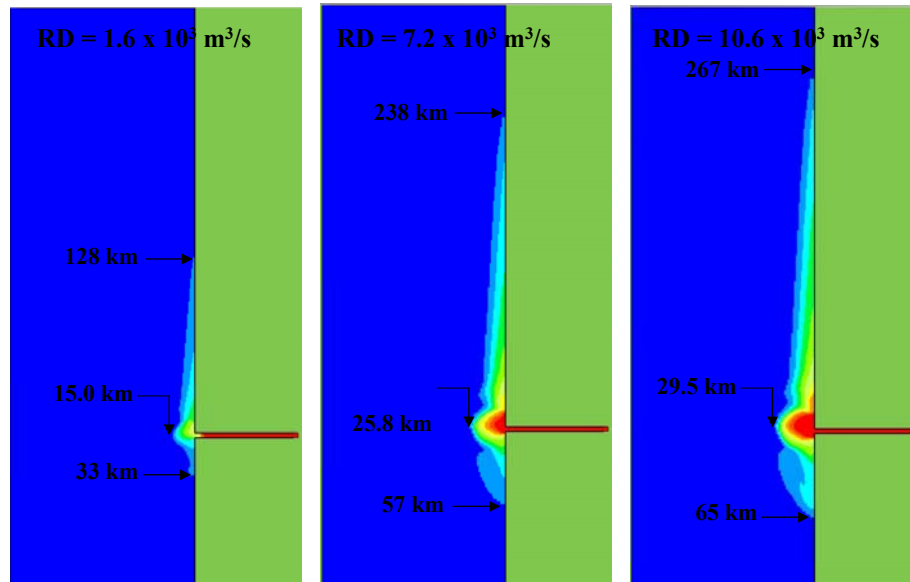


Figure 8. Simulated tidal current river discharge interactions in an estuary-coastal-ocean system. The surface river plume is trapped to the northern coast. The overall property of the river plume is a function of river discharge RD in  $\text{m}^3/\text{s}$ . The color scheme shows salinity values between 20.0 and 30.0 ppt with lighter shade representing higher salinity.

## VI. Summary and Conclusion

The formation of trapped river plumes has been investigated by the UnTRIM numerical model. River derived fresh water discharging into an adjacent continental shelf forms a trapped river plume that propagates in a narrow region along the coast. Previous investigations of trapped river plume neglected tidal circulation or down played the importance of tidal circulation in the estuary. In spite of tidal currents being neglected, often the turbulent kinetic energy based closure model was used (such as the Mellor-Yamada 2.5 level turbulence closure). These weak assumptions prompted a complete investigation of the river plume dynamics by considering an estuary-coastal-ocean system driven by tides, river discharge, and stratification. The UnTRIM model allows the use of an orthogonal unstructured grid as the computational mesh, thus fine meshes are used in the entrance region of the estuary and in the region adjacent to the river mouth.

Model results from this study have clearly shown that the formation of the trapped river plume is due to Coriolis acceleration; all other factors would only create conditions conducive to the formation of a trapped river plume. It has shown further that no matter how favorable the ambient flow conditions might be, without the Coriolis acceleration, there will not be any river plume.

Without the presence of Coriolis acceleration the freshwater exits and partially returns back into the estuary in a tidal cycle forming a symmetric freshwater zone near the mouth of the estuary. In the presence of Coriolis acceleration, the high momentum jet exiting from the estuary is turned clockwise (northern hemisphere), and further confined by the coastal shore forming a long and narrow trapped river plume which propagates in the direction of Kelvin waves. The properties of trapped river plume are related to the magnitude of river discharge and the degree of stratification. Within the estuary, typical flooding and ebbing tidal currents evolve in response to incoming tides from the ocean. The net river discharge must be determined by applying a low-pass filter to the tidal volumetric flux fluctuations in a cross-section. The salinity front or the location of 2 ppt in the estuary is shown to be dependent upon river discharge. The complete properties of velocity and salinity distributions in the estuary and in the coastal ocean have been simulated with a fine resolution unstructured grid numerical model, UnTRIM. The model results are in agreement with general features of trapped river plumes reported in the literature. Direct comparisons of these model results with results reported in the literature are not made because the problem setup and formulation are different from those reported in the literature. In this study, the river plume dynamics is formulated on the basis of sound physical arguments. The numerical results are consistent with what would be expected of such a flow process from a physical point of view.

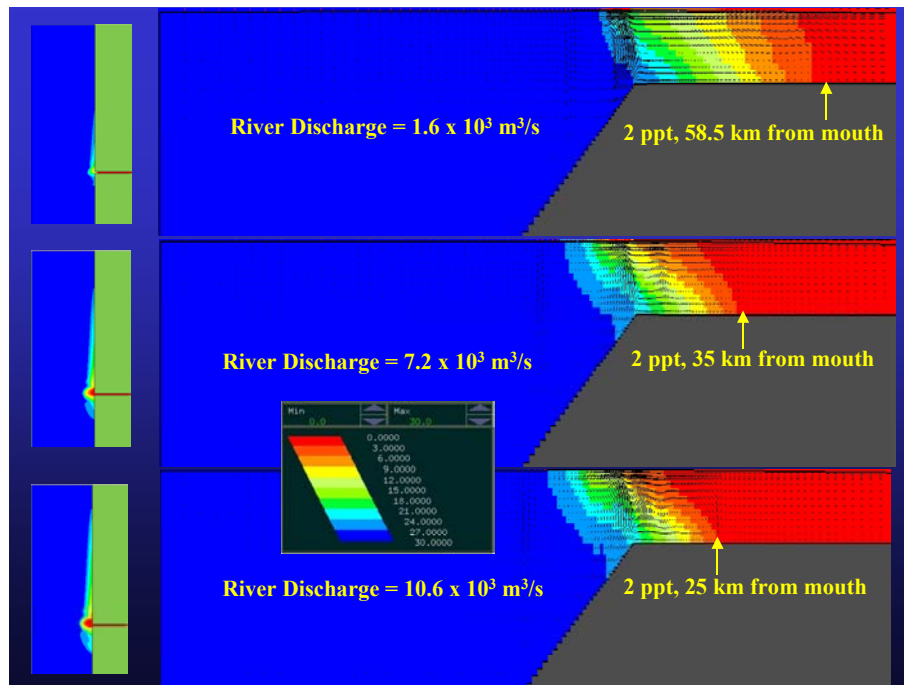


Figure 9. The salinity distributions in a vertical cross-section of the estuary-coastal ocean are shown with the horizontal to vertical scale ratio of 1: 500. The distance of 2 ppt salinity from the river mouth is shown to be inversely proportional to river discharge. The color scheme shows salinity values between 0.0 and 30.0 ppt with lighter shade representing higher salinity value.

**Acknowledgements:** The authors appreciate the detailed editorial suggestions made by an anonymous reviewer.

## VII. References



- Berdeal, I. G., B. M. Hicky, and M. Kawase, 2002, Influence of wind shear and ambient flow on a high discharge river plume, *J. of Geophysical Research*, Vol. 107, No. C9, 3130, doi: 10.1029/2001JC000932, 2002.
- Blumberg, A. F., and G. L. Mellor, 1987, A description of a three-dimensional coastal ocean circulation model, in *Three-Dimensional Coastal Ocean Models*, N. Heaps, Ed., Am. Geophys. Union, p. 1-16.
- Casulli, V., 1990, Semi-implicit finite-difference methods for the two-dimensional shallow water equations, *J. Comput. Phys.*, Vol. 86, p. 56-74.
- Casulli, V. and R. T. Cheng, 1992, Semi-implicit finite difference methods for three-dimensional shallow water flow, *Inter. J. for Numer. Methods in Fluids*, Vol. 15, p. 629-648.
- Casulli, V. and E. Cattani, 1994, Stability, accuracy and efficiency of a semi-implicit method for three-dimensional shallow water flow, *Comput. Math. Appl.*, Vol. 27, p. 99-112.
- Casulli, V. and R.A. Walters, 2000, An unstructured grid, three-dimensional model based on the shallow water Equations. *Inter. J. for Numer. Methods in Fluids*, Vol. 32, p. 331-348.
- Casulli, V. and P. Zanolli, 1998, A three-dimensional semi-implicit algorithm for environmental flows on unstructured grids, *Proc. of Conf. On Num. Methods for Fluid Dynamics*, University of Oxford.
- Casulli, V. and P. Zanolli, 2002, Semi-implicit numerical modeling of non-hydrostatic free-surface flows for environmental problems, *Mathematical and Computer Modeling*, Vol. 36, p. 1131-1149.
- Chao, S. Y. and W. C. Boicourt, 1986, Onset of estuarine plumes, *J. of Physical Oceano.*, Vol. 16, p. 2137-2149.
- Chao, S. Y., 1988, River-forced estuarine plume, *J. of Physical Oceano.*, Vol. 18, p. 72-88.
- Cheng, R. T. and V. Casulli, 1996, Modeling the periodic stratification and gravitational circulation in San Francisco Bay, in *Proceedings of 4-th Inter. Conf. on Estuarine and Coastal Modeling*, Spaulding and Cheng (Eds.), ASCE, San Diego, CA, October 1995, p.240-254.
- Cheng, R. T. and V. Casulli, 2002, Evaluation of the UnTRIM model for 3-D tidal circulation, *Proceedings of the 7-th International Conference on Estuarine and Coastal Modeling*, St.Petersburg, FL, November 2001, p. 628-642.
- Fong, D. A., and W. R. Geyer, 2002, The alongshore transport of freshwater in a surface-trapped river plume, *J. of Physical Oceano.*, Vol. 32, p. 957-972.
- Garvine, R. W., 1987, Estuary plumes and fronts in shelf waters: A layer model, *J. of Phys. Oceanogr.*, Vol. 17, p. 1877-1896.

- Garvine, R. W., 1999, Penetration of buoyant coastal discharge onto the continental shelf: A numerical model experiment, *J. of Physical Oceanogr.*, Vol. 29, p. 1892-1909.
- Garvine, R. W., 2001, The impact of model configuration in studies of buoyant coastal discharge, *J. of Marine Research*, Vol. 59, p. 193-225.
- Hickey, B. M., L. J. Pietrafesa, D. A. Jay, and W. C. Boicourt, 1998, The Columbia River plume study: Substantial variability in the velocity and salinity field, *J. Geophys. Res.*, Vol. 103, p. 10,339-10368.
- Hyatt, J. and R. P. Signell, 2000, Modeling surface trapped river plumes: A sensitivity study, in *Proceedings of the 6-th International Conference on Estuarine and Coastal Modeling*, St.Petersburg, FL, November 3-5, 1999, p. 452-465.
- Kourafalou, V. H., L. Y. Oey, J. D. Wang, and T. N. Lee, 1996, The fate of river discharge on the continental shelf: I. Modeling the river plume and the inner shelf coastal current, *J. Geophys. Res.*, Vol. 101, No. C2, p. 3415-3434.
- Lehfeldt, R. and S. Bloss, 1988, Algebraic turbulence model for stratified tidal flow, in *Physical Processes in Estuaries*, Edited by J. Dronkers and W. van Leussen, p. 278-291, Springer-Verlag.
- Mellor, G. L., and T. Yamada, 1982, Formation of a turbulent closure model for geophysical fluid problems, *Rev. Geophys. Space Phys.*, Vol. 20, p. 851-875.
- Munk, W.H. and E. R. Anderson, 1948, Notes on a theory of the thermocline, *J. Mar. Res.*, Vol. 7, 276-295.
- O'Donnell, J., 1990, The formation and fate of a river plume: A numerical model, *J. Phys. Oceanogr.*, Vol. 20, p. 551-569.
- Oey, L. Y., and G. L. Mellor, 1993, Subtidal variability of estuarine outflow, plume and coastal current: A model study, *J. Phys. Oceanogr.*, Vol. 23, p. 164-171.
- Pacanowski, R. C., and S. G. H. Philander, 1981, Parameterization of vertical mixing in numerical models of tropical ocean, *J. Phys. Oceanogr.*, Vol. 11, p. 16143-16160.
- Rodi, W., 1984, *Turbulence models and their applications in hydraulics - a state of the art review*, 2nd edition, IAHR, The Netherlands, pp.104.
- Uittenbogarrd, R. E., J. A. Th. M. van Kester, and G. S. Stelling, 1992, Implementation of the three turbulence models in TRISULA for rectangular horizontal grids, *Delft Hydraulics Report Z162-22*.
- Yankovsky, A. E., and D. C. Chapman, 1997, A simple theory for the fate of buoyant coastal discharges, *J. Phys. Oceanogr.*, Vol. 27, p. 1386-1401.



Zhang, Q. H., G. S. Janowitz, and L. J. Pietrafesa, 1987, The interaction of estuarine and shelf waters: A model and applications, J. of Physical Oceano., Vol. 17, p. 455-469.